JMEPEG (2014) 23:3058–3068
DOI: 10.1007/s11665-014-1063-z

1059-9495/$19.00

Friction Factor Evaluation Using Experimental and Finite Element Methods for Al-4%Cu Preforms

Wogaso Desalegn, M.J. Davidson, and A.K. Khanra

(Submitted January 8, 2014; in revised form April 27, 2014; published online May 20, 2014)

In this study, ring compression tests and finite element (FE) simulations have been utilized to evaluate the friction factor, *m*, under different lubricating conditions for powder metallurgical (P/M) Al-4%Cu preforms. A series of ring compression tests were carried out to obtain friction factor (*m*) for a number of lubricating conditions, including zinc stearate, graphite, molybdenum disulfide powder, and unlubricated condition. FE simulations were used to analyze materials deformation, densification, and geometric changes, and to derive the friction calibration curves. The friction factor has been determined for various initial relative densities and different lubricating conditions, and a proper lubricant for cold forging of P/M Al-4%Cu preforms is found. Studies show that the use of lubricants has reduced the friction. However, increase in the number of pores in the preforms leads to excessive friction. The FE simulation results demonstrate a shift in the neutral plane distance from the axis of ring specimen, which occurred due to variations in the frictional conditions and initial relative densities. The load requirement for deformation, effective stress, and effective strain induced, and bulging phenomena obtained by FE simulations have a good agreement with the experimental data.

Keywords barreling, FE simulation, friction factor, ring compression test

1. Introduction

Friction occurs in all metal forming operations, and in general, it has significant negative impacts on deformation load and energy requirements, product surface quality, die wear characteristics, and formability of the materials. Excessive friction leads to heat generation and wear of tool surface. Further, it can cause inhomogeneity in deformation, increase the deformation load requirement, and create defects in the work. Investigation of frictional behavior of materials for different metal forming processes under various lubricating conditions is essential for successful transformation of materials into the final desired products. Various authors (Ref 1-4) revealed that friction can be controlled by using suitable lubricants between tool and work piece interfaces. Therefore, evaluation of proper lubricant for powder metallurgical (P/M) parts is quite significant during further processing of the parts into final desired products. Though liquid lubricants have good lubricity for fully dense materials, application of them to P/M parts is a challenge due to the presence of inherent porosity. According to Tabata et al. (Ref 5), open pores on the surface of sintered parts are intercommunicative with the outside atmosphere, and on the other hand, closed pores are individually independent within the matrix. Thus, application of liquid lubricants to P/M preforms with more number of open pores may cause a non-uniform lubricant film at the tool-work piece interfaces.

Ring compression test is widely acceptable method for determining friction factor over the last three decades. It was introduced by Kunogi (Ref 6), and later improved and presented in a useful way by Male and Cockcroft (Ref 7). Since this method utilizes only the measurement of changes in the geometry of the ring specimen without considering determination of mechanical properties of metals, it has been popularly used for evaluation of frictional behavior of metals. Sofuoglu et al. (Ref 8) utilized ring compression test to investigate the effect of material properties, strain rate sensitivity, and barreling on the behavior of friction calibration curves and concluded that the friction calibration curves are notably influenced by material properties and testing conditions, and every material possesses its own distinctive friction calibration curves. Venugopal et al. (Ref 9) conducted ring compression tests on sintered iron preforms of different initial relative densities under various lubricating conditions. They observed that sintered iron preforms exhibit higher friction coefficient as compared to the corresponding wrought 0.5%C steel under similar lubricating conditions. Investigation of friction behavior of sintered iron preforms was carried out by Oh et al. (Ref 10) using ring upsetting and upper-bound approach on the basis of plasticity theory of porous metals. They determined the friction factor (*m*) for different initial relative densities of sintered preforms under various lubricating conditions. They also demonstrated that the friction factor can be obtained from reduction in height and relative density if the initial relative density of the preform is known.

Evaluation of friction factor for TA15 titanium alloy in isothermal process was presented by Zhang et al. (Ref 11) by

Wogaso Desalegn and **M.J. Davidson**, Department of Mechanical Engineering, National Institute of Technology, Warangal 506 004 Andhra Pradesh, India; and **A.K. Khanra**, Department of Metallurgical and Materials Engineering, National Institute of Technology, Warangal 506 004 Andhra Pradesh, India. Contact e-mails: desalegnnitw@gmail.com and desalegnwogaso@nitw.ac.in.

using experimental and finite element (FE) methods, in which the latter was used to elaborate the friction calibration curves and evaluate geometric changes. The results revealed that the interfacial friction is significantly dependent on the material properties and forming conditions, namely, loading speed, temperature, and type of lubricants used. Shahriari et al. (Ref 12) conducted experimental study and 3D FE simulations to determine friction factor of Nimonic 115 superalloy in hot forging conditions. Babu Rao et al. (Ref 13, 14) adopted ring compression test and FE analysis on aluminum ring specimens to investigate the effect of friction on metal flow behavior. The study of ring compression test using physical modeling and FE simulations was also presented by Robinson et al. (Ref 15), and they showed that the FE simulations provide accurate and effective results for the analysis of frictional behavior of metals. Tan et al. (Ref 16) conducted experimental, theoretical, and FE analysis of friction for aluminum alloy AA6082 at various normal pressures using different ring geometries. FE simulation was also used by Zhu et al. (Ref 17) for determination of friction factor for Ti-6Al-4V titanium alloy in hot forging by means of ring compression test. They carried out detailed analysis of metal flow behavior and changes in the geometry of the material for different heat transfer coefficients. Thus, ring compression test combined by FE simulations is expected to give detailed and accurate results of friction and deformation behavior for P/M materials.

The literature studies related to the evaluation of frictional behavior using ring compression test and FE simulations for P/M aluminum-copper composites are limited. In addition, aluminum-copper composites are widely used in major industrial applications, namely, air-craft structures, rivets, hardware, truck wheels, and screw-machine products as described by Mondolfo et al. (Ref 18). Thus, it is quite significant to study the frictional behavior of P/M Al-4%Cu preforms using experiment and FE simulation for different initial relative densities and lubricating conditions.

2. Experimental Details

Sintered Al-4%Cu preforms were prepared using P/M route from atomized pure aluminum and copper powders of each −325 mesh size. The aluminum powder is 99% pure with a maximum of 0.53% insoluble impurity limit. The purity level of copper powder is 99%, and it has a maximum of 0.5 and 0.03% impurities of iron and heavy metal (Pb), respectively. The SEM photographs of aluminum and copper powder are shown in Fig. 1(a) and (b). The powder particles are flake in shape which is the typical nature of atomized metal powder. Al-4%Cu compacts with initial relative densities, namely, 0.75, 0.85, and 0.9 were made by using recommended compaction pressures. Zinc stearate was used for lubricating die, punch, and butt to reduce interface friction. The powder compacts were sintered in a tubular furnace at 550 ± 10 °C for a holding time of 45 min in argon-gas atmosphere. Immediately after the completion of sintering schedule, the compacts were allowed to cool to room temperature inside the furnace by switching off the furnace power source. The density of the sintered compacts was ascertained by Archimedes's principle at room temperature with an accuracy of ±1%.

The ring compression specimens were prepared by machining the sintered preforms to standard ring compression specification of outer diameter: inner diameter: height ratio of 6:3:2 (20:10:6.67 mm). To ensure similar surface roughness, the same machining operations were applied to both upper and

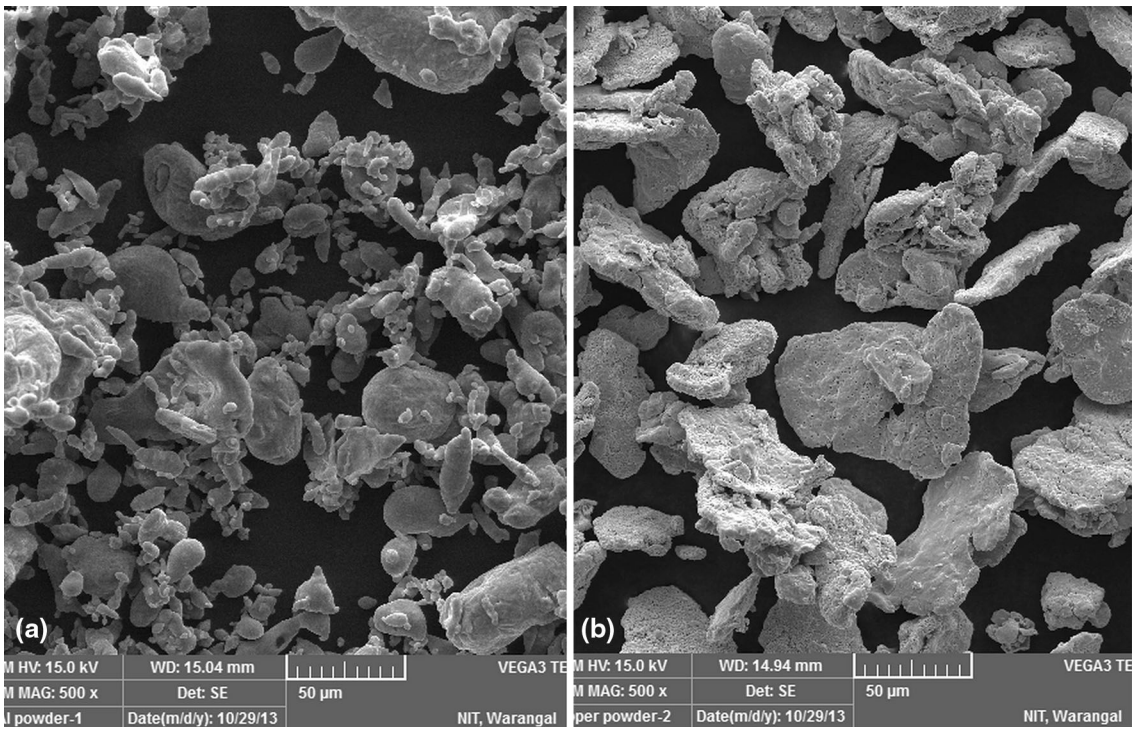

Fig. 1 (a) The SEM photograph of aluminum powder. (b) The SEM photograph of copper powder

lower surfaces of the ring specimens. Both surfaces of the ring specimen were polished with emery paper. The ring compression test was carried out between two parallel flat mirror finished open dies of 50 ton capacity hydraulic press with a ram speed of 0.5 mm/s. The tests were performed on six specimens for each lubricating conditions and initial relative densities. Figure 2 shows the dimensions of the ring specimen, namely, bulged diameter (D_{bl}), diametrial expansion of the hole (D_{eh}), diametrial contraction of the hole (D_{ch}), and height of the preform (H_f) which were recorded before and after deformation for different experimental conditions. To get accurate results, each experiment was repeated three times for all experimental conditions. The various lubricating conditions adopted in this investigation were zinc stearate, graphite, molybdenum disulfide powder, and unlubricated condition, respectively.

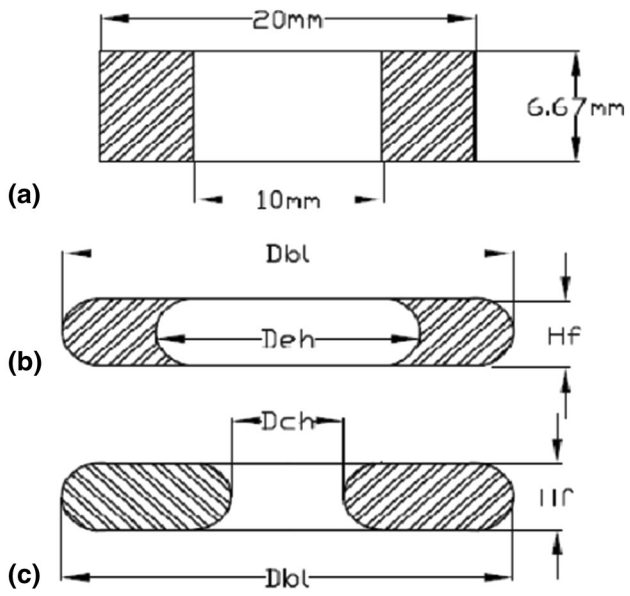

Fig. 2 Ring specimen geometry (a) before deformation (b) deformed under low frictional condition (c) deformed under high frictional condition

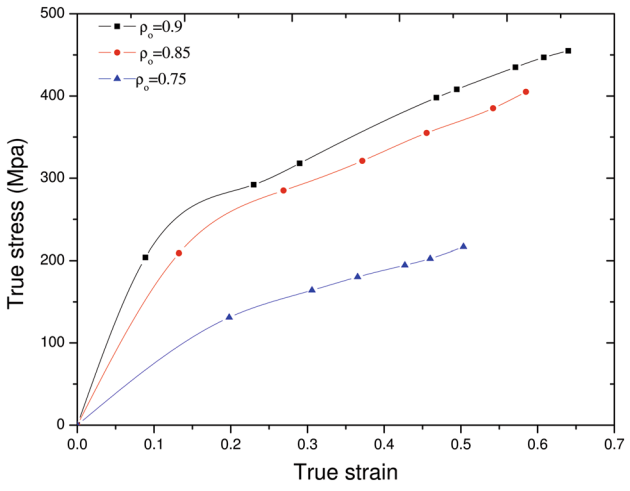

Fig. 3 True stress-strain curve for sintered Al-4%Cu preforms for initial relative densities of 0.9, 0.85 and 0.75 respectively

3. Result and Discussion

3.1 Friction Calibration Curve and Friction Factor (m)

In this work, an attempt was made to determine the friction factor (m) for various lubricating conditions by measuring the change in the inner diameter (%) and reduction in height (%) of the ring specimens. The properties of materials were determined using compression test on sintered cylindrical Al-4%Cu preforms of aspect ratio 0.5 (height: diameter) and for different

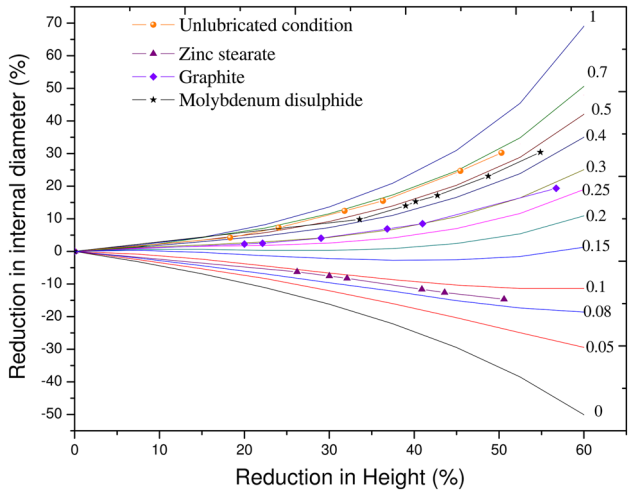

Fig. 4 Friction calibration curve for experimental results fitted against Male and Cockcroft calibration curve for initial relative density, ρ_o = 0.9

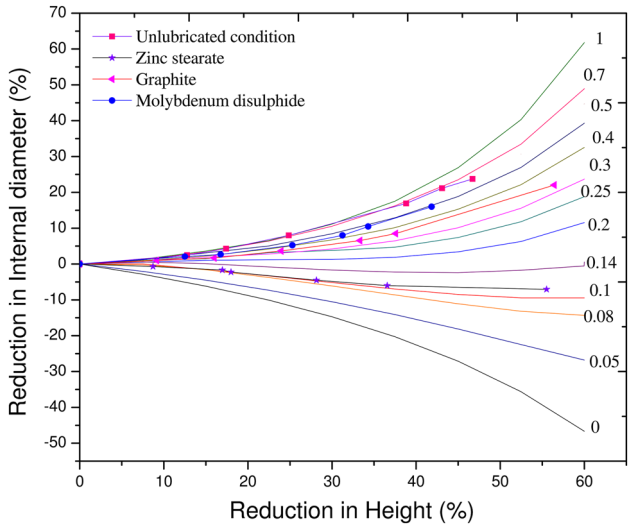

Fig. 5 Friction calibration curve for experimental results fitted against Male and Cockcroft calibration curve for initial relative density, ρ_o = 0.85

initial relative densities of 0.75, 0.85, and 0.9, respectively. The friction calibration curves were derived by using FE method software (DEFORM 2D) by incorporating the properties of material as input.

The true stress-true strain curves of sintered Al-4%Cu preforms of different initial relative densities are generated from the compression test and are illustrated in Fig. 3. The flow stress equations of the Al-4%Cu preforms were obtained by fitting the properties of material, specifically, apparent strain hardening exponent (n_a) and apparent strength coefficient (K_a), into the general flow stress equation for porous materials (Ref 19), $\sigma = K_a \in^{n_a}$, which is equivalent to the general Ludwik equation for fully dense materials. The flow-stress equations thus obtained are given as $\sigma = 546 \in^{0.41}$, $\sigma = 504 \in^{0.44}$ and $\sigma = 313 \in^{0.54}$ for initial relative density of 0.9, 0.85, and 0.75, respectively. The apparent strain hardening exponent, n_a, is found to be increasing with decrease in initial relative density. This is due to higher work hardening phenomena observed in lower initial relative density preforms during deformation as a result of dominant effect of densification. On the other hand, the strength coefficient is increasing with increase in the initial relative density of the preforms. During deformation, preforms with lower initial relative density undergo more deformation.

Figure 4, 5, 6 present the friction calibration curves showing the effect of initial relative density on friction factor (m) for different lubricating conditions. The friction factor was determined by plotting reduction in inner diameter (%) and reduction in height (%) of the ring specimen and made to fit against Male and Cockcroft friction calibration curves (Ref 6).

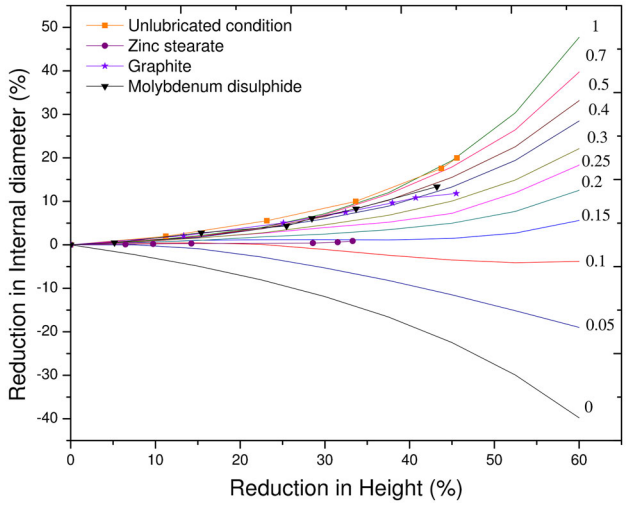

Fig. 6 Friction calibration curve for experimental results fitted against Male and Cockcroft calibration curve for initial relative density, $\rho_o = 0.75$

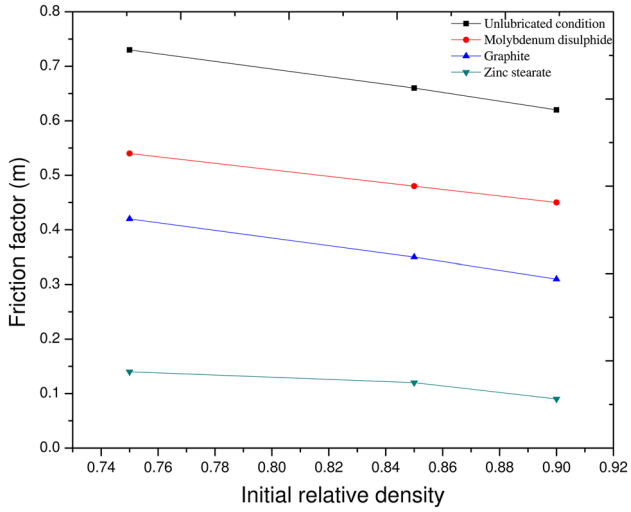

Fig. 7 Variation of friction factor (m) with respect to initial relative density for different lubricating conditions

Table 1 Variations of the relative density under different lubricating conditions for preforms with initial relative density of 0.75, 0.85, and 0.9 deformed to the same level of height reduction (45%)

			Relative density after 45% height reduction		
Initial relative density (ρ_o)	Lubricating condition	Friction factor (m)	Minimum value (ρ_{min})	Maximum value (ρ_{max})	Variation (%)
0.9	Zinc stearate	0.09	0.97	0.98	1.03
	Graphite	0.31	0.95	0.99	4.21
	Molybdenum disulfide	0.45	0.93	0.99	6.45
	Unlubricated condition	0.62	0.92	0.99	7.61
0.85	Zinc stearate	0.12	0.94	0.98	4.26
	Graphite	0.35	0.92	0.99	7.61
	Molybdenum disulfide	0.48	0.9	0.99	9.09
	Unlubricated condition	0.66	0.88	0.99	12.5
0.75	Zinc stearate	0.14	0.89	0.96	7.87
	Graphite	0.42	0.85	0.99	16.47
	Molybdenum disulfide	0.54	0.84	0.99	17.86
	Unlubricated condition	0.73	0.82	0.99	20.73

Fig. 8 Photographs of deformed ring specimens under different lubricating conditions to height reduction of 45% for initial relative densities of (a) 0.9 (b) 0.85 and (c) 0.75

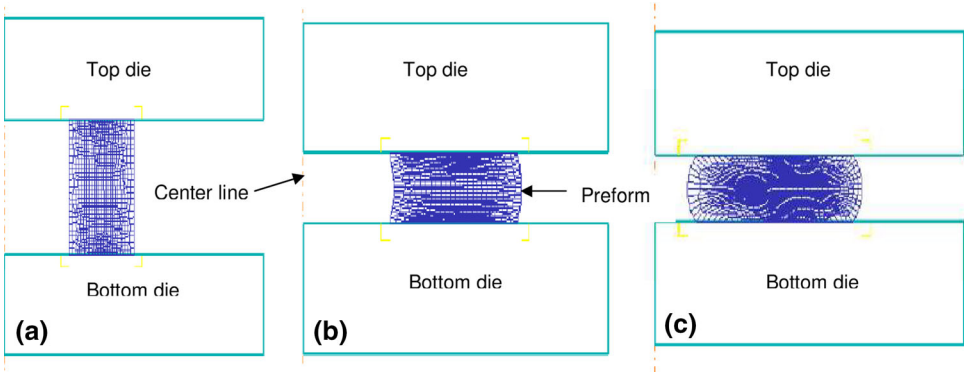

Fig. 9 Finite element method modeling of ring compression test (a) before deformation, (b) after deformation under low friction, (c) after deformation under high friction

From the general observation of Fig. 4-6, the interfacial friction is considerably lower, which is secured by the use of lubricants, namely graphite, molybdenum disulfide, and zinc stearate powder irrespective of the initial relative density. The values of the friction factor, m, for different initial relative densities and lubricating conditions are given in Table 1.

For unlubricated conditions, the contraction of the ring hole or barreling was higher due to more flow of metals to the middle part of the preforms and, consequently, it resulted in increased bulging phenomena. Preforms deformed using zinc stearate lubricant show the largest hole expansion or mushrooming effect irrespective of the initial relative density. The reason is decrease in sticking nature of the material with the tool at the interfaces, which determines the extent of particle-tool interaction.

Figure 7 shows the variation in the friction factor with respect to initial relative density for different lubricating conditions. The friction factor, m, is increasing with decrease

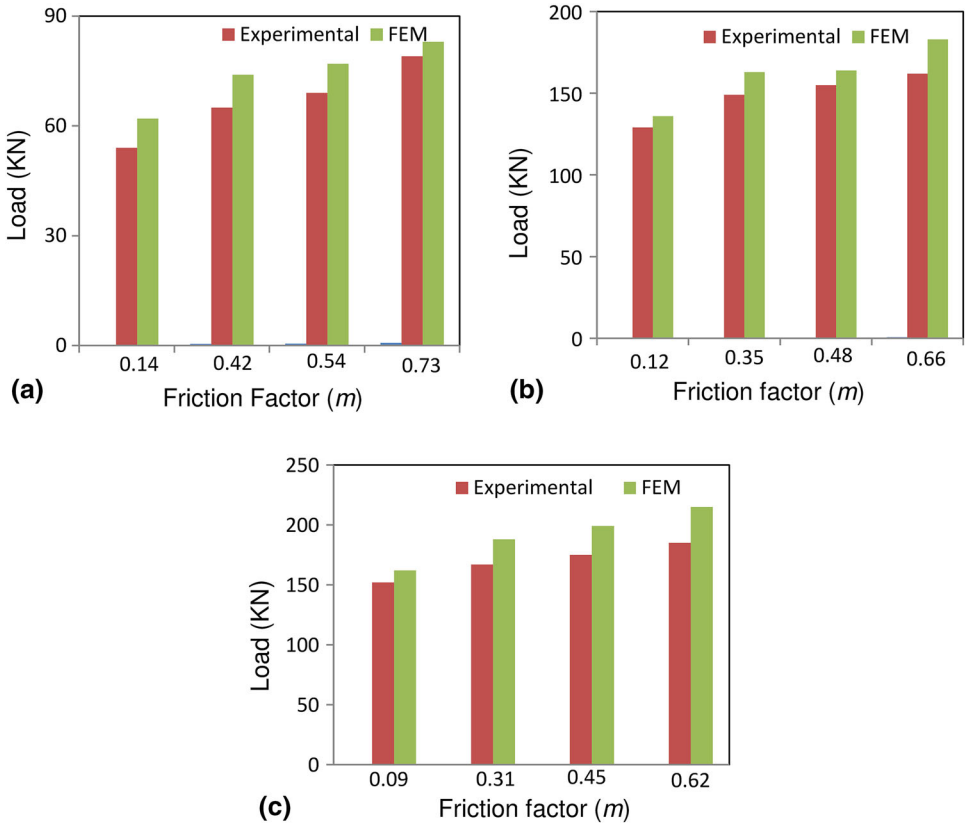

Fig. 10 Variation of experimental and FEM load requirements with respect to friction factor for preforms of initial relative density (a) 0.75, (b) 0.85, and (c) 0.9

in the initial relative density for all lubricating conditions. This is due to higher work hardening effect for lower density preforms. The pores act as a damper which restricts the flow of metals at tool-work piece interfaces; instead, it increases the dead metal zone formation, and hence the friction factor is increased. Zinc stearate was found to be a proper lubricant with least friction factor (m), namely, 0.09, 0.12, and 0.14 for initial relative densities of 0.9, 0.85, and 0.75, respectively. Because of the high friction generated between tool and work piece interfaces for lower initial relative density preforms and unlubricated conditions, the lateral flow of metals at the tool-work piece interfaces is restricted, and consequently, the bulging phenomena are higher. Figure 8a-c shows the photographs of P/M Al-4%Cu ring specimens with initial relative density of 0.9, 0.85, and 0.75, respectively, deformed under different lubricating conditions.

3.2 Finite Element Simulation

The FE modeling of ring compression test carried out using DEFORM 2D software is illustrated in Fig. 9 for different frictional conditions. An axisymmetric formulation of the billet was considered during modeling; hence 2D modeling in Fig. 9 represents only one quarter of the ring specimen. A quadrilateral nodded, 1000 elements with size ratio of 3 were used to mesh the billet. The specimen was modeled as a porous material with initial relative densities given as 0.9, 0.85, and 0.75, respectively. The deformation was carried out for different lubricating conditions, namely, molybdenum disulfide, graphite, zinc stearate powder, and unlubricated condition. The friction factor was determined by fitting the experimental results on Male and Cockcroft calibration curves which are constructed by DEFORM 2D software. The billet was deformed to the same level of height reduction for all initial relative densities under various lubricating conditions.

Comparisons between the load requirement for deformation obtained from experiment and FE simulation are illustrated in Fig. 10a-c for different initial relative densities. It is clearly evident that the load required for deformation increases with increase in the friction factor for all the cases of initial relative densities. This is due to increase in adherence of the material with the tool which restricts the metal flow at the tool-work piece interfaces. As a result, the interfacial friction between the tool and specimen increases.

The non-uniformity in density distribution and metal flow is also more prominent when the friction factor increases. Table 1 shows the relative density variations (%) for preforms deformed

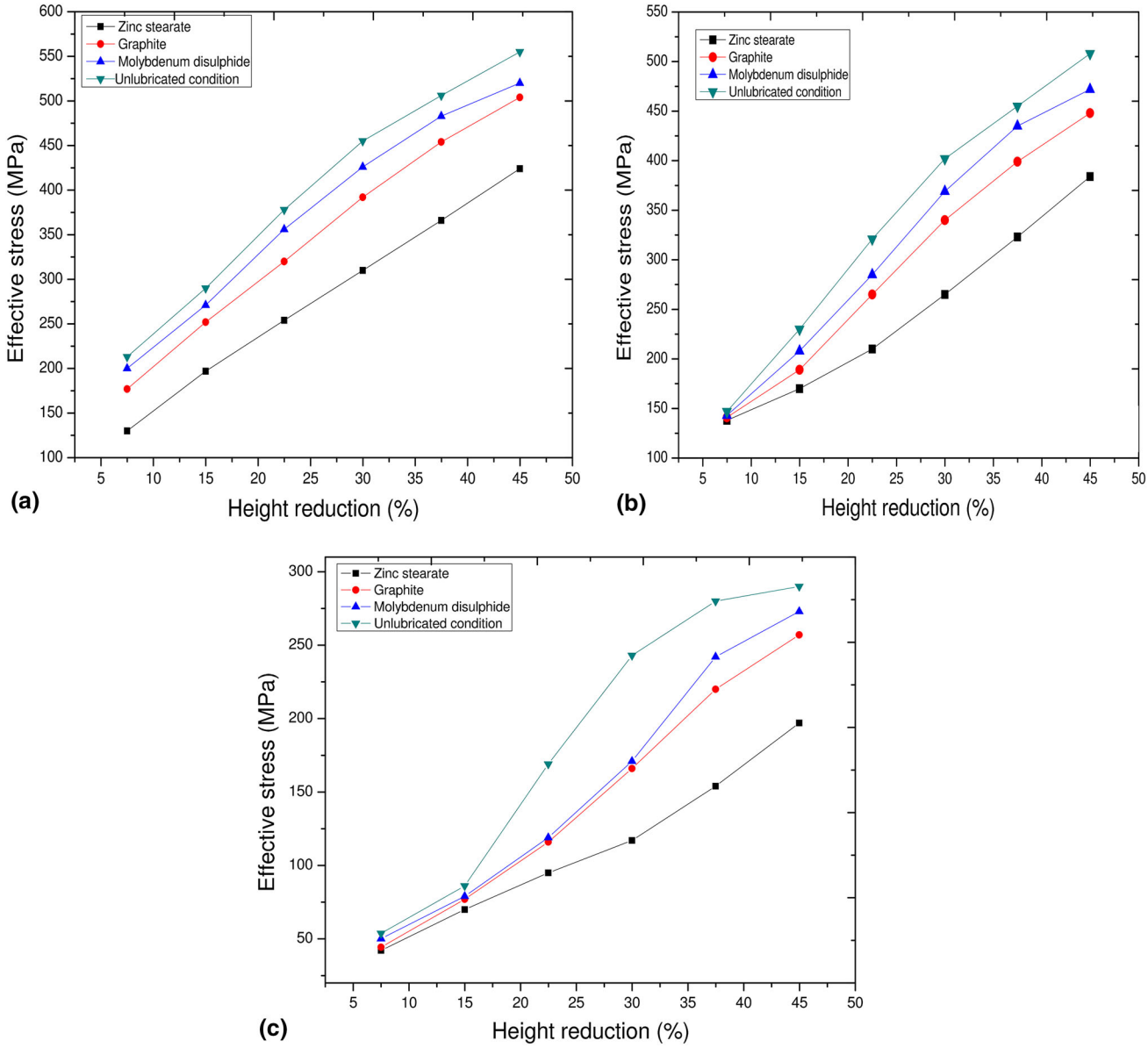

Fig. 11 Variation of effective stress with respect to height reduction (%) under different lubricating conditions for preforms with initial relative density of (a) 0.9, (b) 0.85, and (c) 0.75

to the same level of height reduction (45%) under different lubricating conditions. The non-uniformity in the densification is increasing when the friction factor increases irrespective of the initial relative densities. Preforms deformed using zinc stearate lubricant showed a minimum variation in density distribution, namely, 1.03, 4.26, and 7.87% for initial relative density of 0.9, 0.85, and 0.75, respectively. The variation in density is higher for lower initial relative density preforms. The densification at the bulged end surface of the preform is low due to free mobility of particles to the region which is the influence of the tensile hoop stress developed in the preform.

Variation in effective stress and effective strain with respect to height reduction (%) was analyzed for different experimental conditions using FEM software (DEFORM 2D), and illustrated in Fig. 11 and 12, respectively. The effective stress and effective strain are continuously increasing with increase in the height reduction and friction factor for all the cases of initial relative densities. The rate of increase in effective stress is low at the initial stage of deformation due to less resistance of the material to deformation as a more number of pores are present. With further increase in deformation, the rate of increase in the effective stress is higher due to combined effect of densification

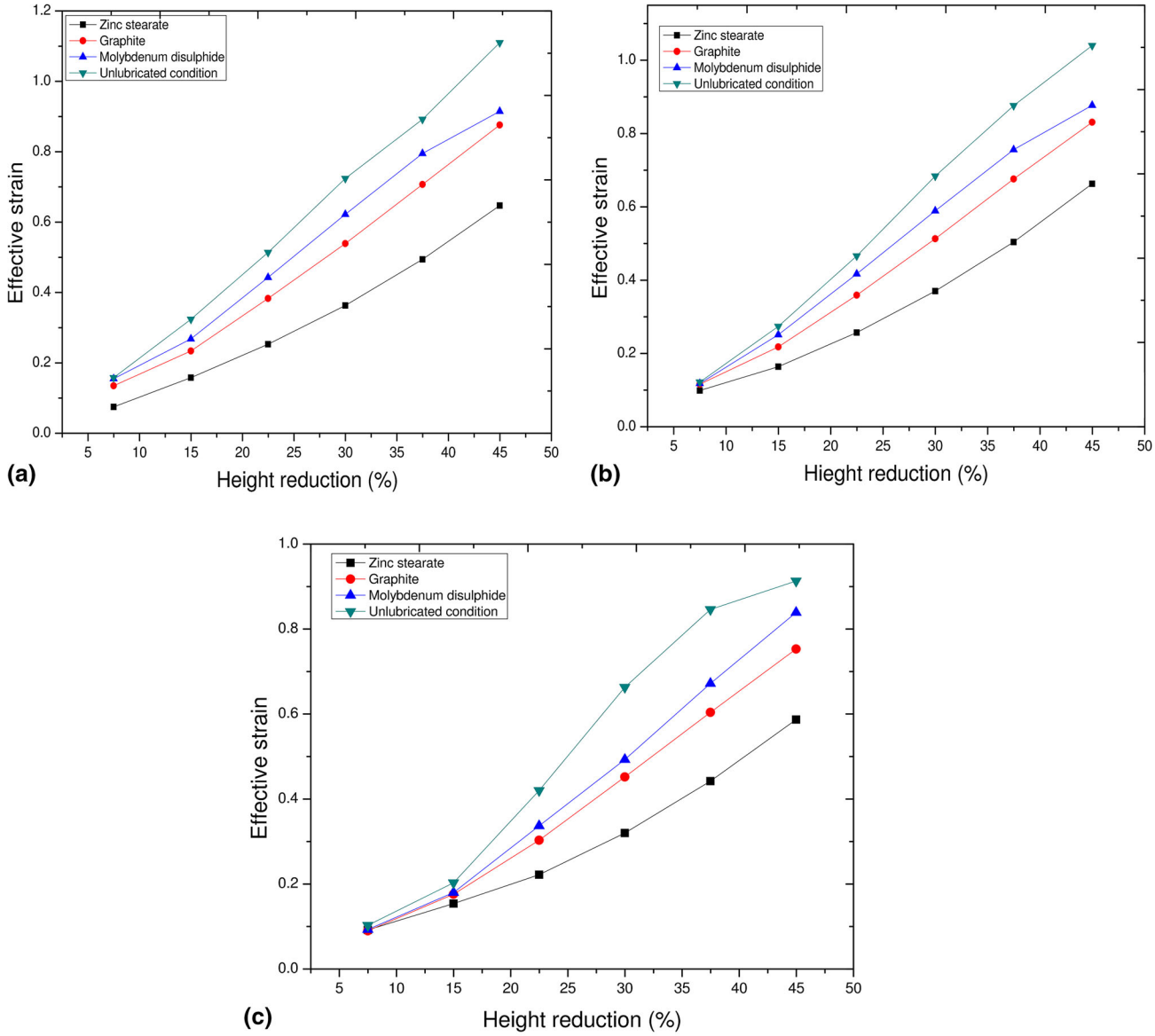

Fig. 12 Variation of effective strain with respect to height reduction (%) under different lubricating conditions for preforms with initial relative density of (a) 0.0.9, (b) 0.85, and (c) 0.75

hardening and matrix work hardening. The effect is more eminent for preforms with lower initial relative densities.

During deformation, there is a volume change, and as a result, the movement of particles is not uniform in different regions of the specimens. The movement of particles shifts either inside or outside of the neutral plane depending up on the interfacial friction conditions. Along the neutral plane, the velocity of the particles is near to zero as shown in Fig. 13.

Figure 13 clearly illustrates the velocity profile at 45% height reduction and shifts in neutral plane with change in friction factor. The distance of the neutral plane from the axis of the ring is increasing with increase in the friction factor for all the cases of initial relative densities. The flow of particles toward inside surface of the ring is notably high for preforms deformed under unlubricated condition which increases the barreling phenomena. The velocity of the particles at the top and bottom interfaces of tool-work piece is low due to sticking nature of the material which restricts the metal flow. Figure 14a-c shows the variations of neutral plane distance with respect to friction factor (m) for various initial relative densities at 45% height reduction.

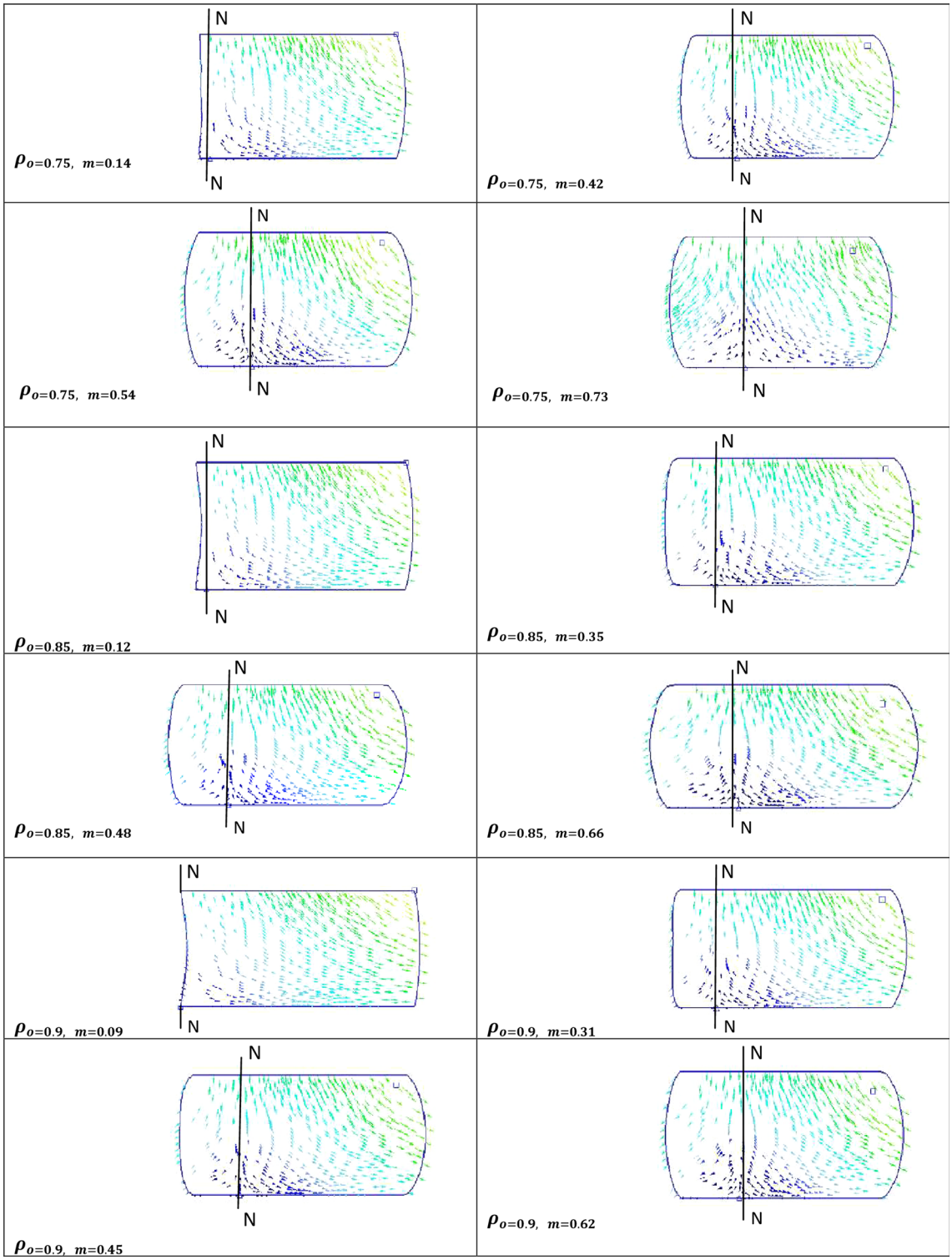

Fig. 13 The velocity distribution and shift in the neutral plane from the axis of the ring under different friction condition of initial relative density 0.75, 0.85, and 0.9 for 45% height reduction

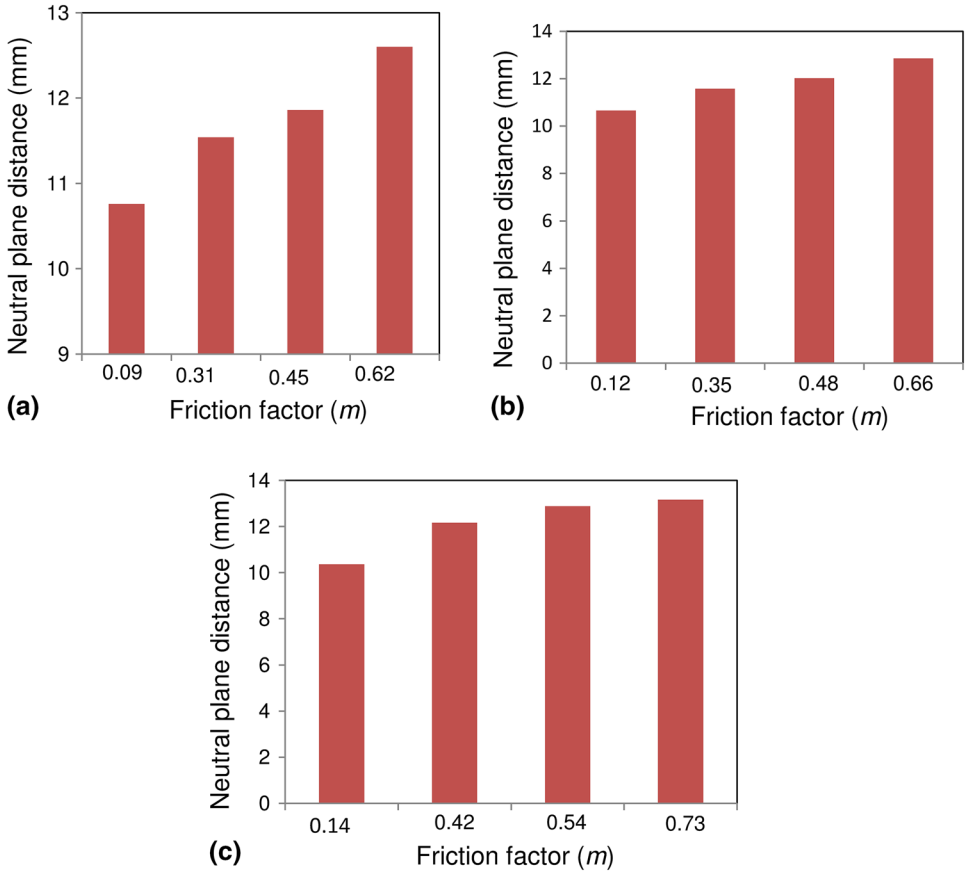

Fig. 14 Variation in the neutral plane distance with friction factor for preforms with initial relative density (a) 0.9, (b) 0.85, and (c) 0.75 for 45% height reduction

4. Conclusion

Based on the experimental and FE simulation results of ring compression test on P/M Al-4%Cu preforms of different initial relative densities under various lubricating conditions, the following conclusions have been drawn:

- Zinc stearate is found to be proper lubricant for successful transformation of P/M Al-4%Cu preforms to the final desired part as it results in a minimum deformation load requirement, induced effective stress and strain, bulging phenomena, and density variations
- The friction factor (m) is increasing with decrease in the initial relative density due to more work hardening phenomena which are the effect of both densification and matrix work hardening
- The contraction of the hole or barreling is increasing with increase in the friction factor (m) where as mushrooming effect or hole expansion is increasing with decrease in the friction factor (m)
- The non-uniformity of density distribution is higher with increase in the friction factor and decrease in the initial relative density
- The shift of neutral plane distance from the axis of the ring is increasing with increase in the friction factor. The effect is more prominent for preforms with lower initial relative density.
- The FE simulation provided detailed and effective results in the analysis of metal flow pattern, density gradient, load requirements, and geometric changes which were in a good agreement with the experimental results. Thus, ring compression test combined with FE simulation is simple and accurate tool to investigate the friction behavior of P/M materials.

References

1. D. Shahriari, M.H. Sadeghi, G.R. Ebrahimi, and K.T. Kim, Effects of Lubricant and Temperature on Friction Coefficient During Hot Forging of Nimonic 115 Superalloy, *Kovove Mater.*, 2011, **49**, p 375–383
2. Ryo Matsumoto and Kozo Osakada, Measurement of Friction in Cold Upsetting with Mist Lubrication, *Mater. Trans.*, 2004, **45**(9), p 2891–2896
3. E. Rajesh, and M. SivaPrakash, Analysis of Friction Factor by Employing the Ring Compression Test Under Different Lubricants, *Int. J. Sci. Eng. Res.*, 2013, **4**(5), p 1163–1171
4. M.S. Zaamout and J.A. Makhadmi, Interface Friction Factor for Commercial Purity Aluminum Forged Under Dry and Lubricated, Umm Al-Qura Univ, *J. Sci. Med. Eng.*, 2007, **19**(2), p 191–202
5. T. Tabata and S. Masaki, Determination of the Coefficient of Friction in Forging of Porous Metals from Ring Compression, *Int. J. Mech. Sci.*, 1978, **20**, p 505–512
6. M. Kunogi, Reports of the Scientific Research Institute, *Tokoyo*, 1954, **30**, p 63

7. A.T. Male, and M.G. Cockcroft, A Method for the Determination of the Coefficient of Friction of Metals Under Bulk Plastic Deformation, *J. Inst Met*., 1964/1965, **93**, 38–46
8. H. Sofuoglu and J. Rasty, On the Measurement of Friction Coefficient Utilizing the Ring Compression Test, *Tribol. Int.*, 1999, **32**, p 327–335
9. P. Venugopal, S. Venkatraman, R. Vasudevan, and K.A. Padmanabhan, Ring Compression Tests on Sintered Iron Preforms, *J. Mech. Work. Technol.*, 1988, **16**, p 51–64
10. H.K. Oh and J.H. Mun, An Analysis of the Ring Upsetting of Sintered Material, *J. Mech. Work. Technol.*, 1984, **9**, p 279–290
11. D.-W. Zhang, H. Yang, H.-W. Li, and X.-G. Fan, Friction Factor Evaluation by FEM and Experiment for TA15 Titanium Alloy in Isothermal Forming Process, *Int. J. Adv. Manuf. Technol.*, 2012, **60**, p 527–536
12. D. Shahriari, A. Amiri, and M.H. Sadeghi, Study on Hot Ring Compression Test of Nimonic 115 Superalloy Using Experimental Observations and 3D FEM Simulation, *J. Mater. Eng. Perform.*, 2010, **19**, p 633–642
13. J.B. Rao, S. Kamaluddin, J.A Rao, M.M.M. Sarcar and N.R.M.R Bhargava, Determination of Friction Factor During Cold Upset Forging and Its Finite Element Analysis. *J. Inst. Eng. (India), Metall. Mater. Eng. Div.*, 2011, **92**, 9–15
14. J.B. Rao, S. Kamaluddin, and N.R.M.R. Bhargava, Optical Strain Measurements and Its Finite Element Analysis of Cold Workability Limits of Pure Aluminium, *Int. J. Eng. Sci. Technol.*, 2010, **2**(12), p 1–13
15. T. Robinson, H. Ou, and C.G. Armstrong, Study on Ring Compression Test Using Physical Modeling and FE Simulation, *J. Mater. Process. Technol.*, 2004, **153-154**, p 54–59
16. X. Tan, P.A.F. Martins, N. Bay, and W. Zhang, Friction Studies at Different Normal Pressures with Alternative Ring-Compression Tests, *J. Mater. Process. Technol.*, 1998, **80-81**, p 292–297
17. Y. Zhu, W. Zeng, X. Ma, Q. Tai, Z. Li, and X. Li, Determination of the Friction Factor of Ti-6Al-4V Titanium Alloy in Hot Forging by Means of Ring-Compression Test Using FEM, *Tribol. Int.*, 2011, **44**, p 2074–2080
18. L.F. Mondolfo, *Aluminum alloys: Structures and Properties*, Butterworths, London, 1976
19. P. Venugopal and S. Venkatraman, Some Uses of n_a and K_a in the Prediction of Cold Extrusion Forces of Sintered Powder Metallurgical Preforms, *J. Mech. Work. Technol.*, 1988, **17**, p 113–117